

ENERGY FLOW AND TRANSIENTS IN THE ALVAREZ STRUCTURE

H. G. Hereward and P. Lapostolle

CERN, Geneva (Switzerland)

1. INTRODUCTION

When the Alvarez structure is used for accelerating protons it is operated at the end of its pass-band, where its group velocity is zero. An understanding of the flow of energy in such a structure will be especially important if it is considered for future high-intensity linacs, in which substantial amounts of extra power will be required to compensate for beam loading. In section 2 we give some examples in which rather elementary methods are applied to a transmission-line equivalent circuit (1) while in sections 3 and 4 a more complete treatment is based on a cylindrical waveguide model (2-3).

2. THE TRANSMISSION-LINE MODEL

We represent the Alvarez structure by the circuit shown in Fig. 1.

Near the zero-mode the phase shift per cell is small and the wave equation becomes.

$$\frac{d^2 I}{dx^2} = -L C_s (\omega^2 - \omega_0^2) I \quad [1]$$

where L and C_s represent respectively the series inductance and shunt capacitance per unit length, ω_0 is the resonant or "cut-off" frequency of the structure, and I stands for the current flowing along the drift-tubes and capacitatively from one to the next, a time dependence $\exp j\omega t$ being always understood.

This wave equation readily gives such well-known results as the longitudinal mode spectrum of a cavity, the evanescent modes when $\omega < \omega_0$, the vanishing of group velocity at $\omega = \omega_0$.

Four cases in which there are simple solutions of [1] with some flow of energy are outlined below, and given in more detail in (1).

— Energy is fed into a cavity at one end, travels the whole lossless length of the structure, and is withdrawn by a resistive wall, or coupling loop

etc., at the far end. A steady state at $\omega = \omega_0$ is taken. Then the general solution of [1] is

$$I = A + Bx \quad [2]$$

and the boundary condition at the far end of the cavity determines B/A .

— Slow sinusoidal modulation of the amplitudes in the cavity may be studied by superposing a centre frequency ω_0 and two close side-bands.

— Our equivalent circuit of Fig. 1 can be generalized to include distributed losses by replacing the inductors by impedances $j\omega L + R$, and solved for the steady state at ω_0 .

— A lossless cavity in which the amplitude is increased linearly with time can be studied by successive approximation.

One finds in every case that the flow of energy is associated with a gradient of phase along the cavity, given by

$$\frac{d\phi}{dx} = -\omega L C_s \frac{\text{Rate of energy flow}}{\text{Stored energy per unit length}} \quad [3]$$

and that any amplitude variations along the length of the cavity are typically less important than this phase gradient.

Comparison of the fields corresponding to L and C_s with those in a coaxial line shows that one may put

$$L C_s = K c^{-2} \quad [4]$$

where c is the velocity of light, and that one may expect K to be greater than one, but not by a large factor.

3. CYLINDRICAL WAVEGUIDE MODEL

a) Lossless

Another simple representation of the structure (2) is a circular waveguide of radius a loaded

by a dielectric of constant K. For the E₀₁ mode the longitudinal electric component has the form:

$$E_x = J_0(k_r a) f(x, t) \quad [5]$$

where

$$k_r a = 2,405, \quad [6]$$

the first root of the Bessel function J₀; and under transient conditions one has

$$\frac{\partial^2 f}{\partial x^2} - \frac{K}{c^2} \frac{\partial^2 f}{\partial t^2} - k^2 f = 0 \quad [7]$$

b) Lossy

If losses introduce only a slight perturbation to distribution [5] and are such that field components in the metal drop exponentially like Hankel functions with large arguments, equation [7] can be replaced by

$$\frac{\partial^2 f}{\partial x^2} - \frac{K}{c^2} p^2 f - k^2 f = \frac{2k_1 K}{2,405 c^2 \sqrt{\mu\gamma}} p^{3/2} f \quad [8]$$

where $p = \partial/\partial t$ and γ is the conductivity of the walls. The fractional power of p can be eliminated by squaring symbolically both sides; this gives a

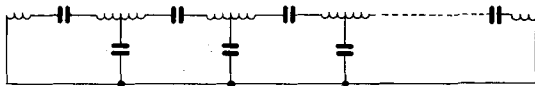


Fig. 1 - Equivalent circuit for the Alvarez structure. The drift tubes are represented by inductors, with capacitance between them and to ground.

partial derivative equation of the fourth order*. The order may be kept to the second by the assumption that the spectrum of f contains only frequencies close to ω_0 , which allows us to replace p by $j\omega_0$ in the perturbation term on the right. Then, separating the real and imaginary parts and keeping p in one of them we find:

$$\frac{\partial^2 f}{\partial x^2} - \frac{K}{c^2} \frac{\partial^2 f}{\partial t^2} - k^2 f - 4\pi K \epsilon R \frac{\partial f}{\partial t} = 0 \quad [9]$$

where R is the longitudinal r.f. resistivity of the walls, and k is now given by $k(a + \delta/2) = 2,405$, δ being the usual skin depth. Introducing the

(*) In fact eq. (8) already assumes that the losses are small. Otherwise other terms should be included raising the order of the equation to the sixth.

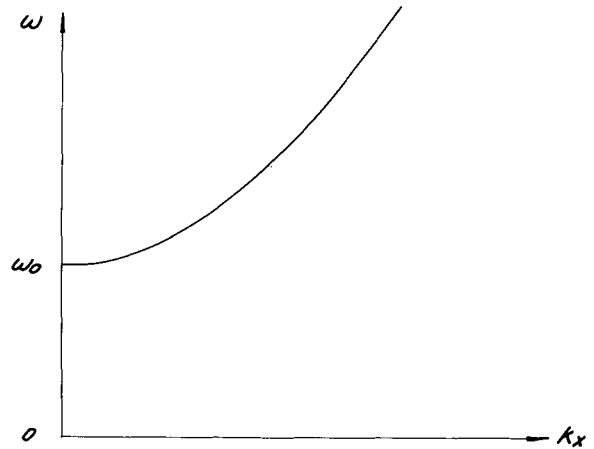


Fig. 2 - Dispersion curve for a circular waveguide.

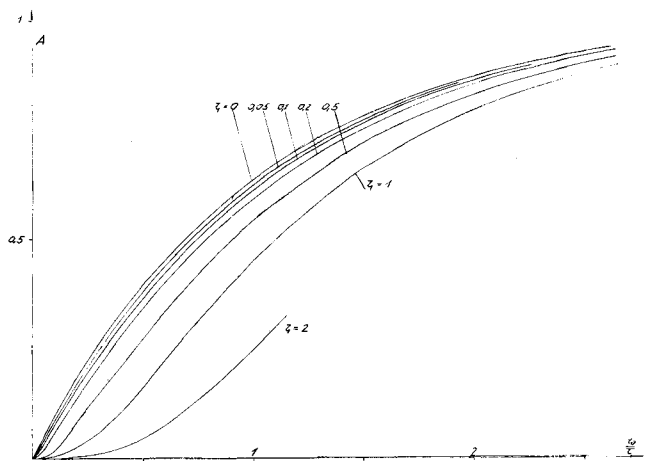


Fig. 3 - Amplitude response along an infinite waveguide at cut-off (amplitude normalized for A = 1 at $t = \infty$).

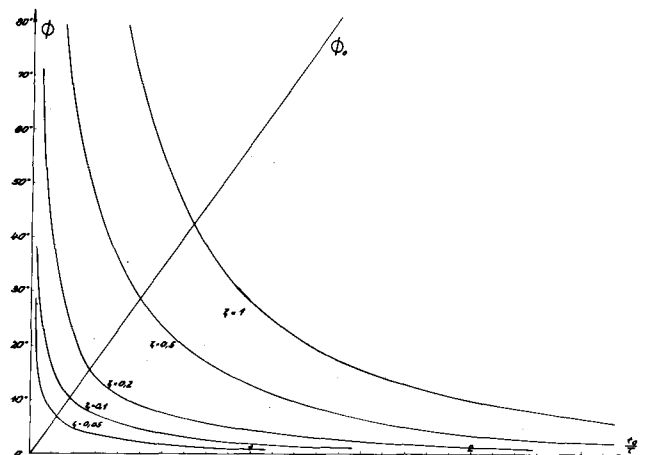


Fig. 4 - Phase response along an infinite waveguide at cut-off (phase normalized for $\phi = 0$ at $t = \infty$).

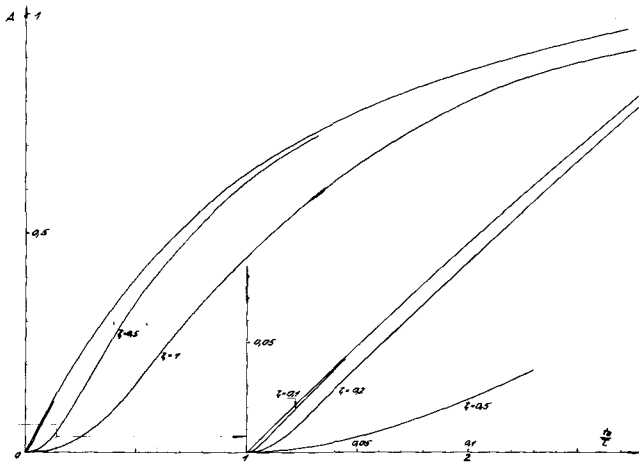


Fig. 5 - Amplitude response at the end of a cavity at cut-off (amplitude normalized for $A = 1$ at $t \rightarrow \infty$).

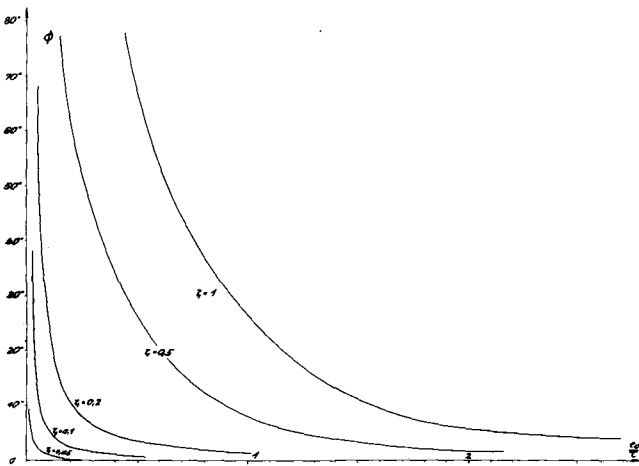


Fig. 6 - Phase response at the end of a cavity at cut-off (phase normalized for $\phi = 0$ at $t \rightarrow \infty$).

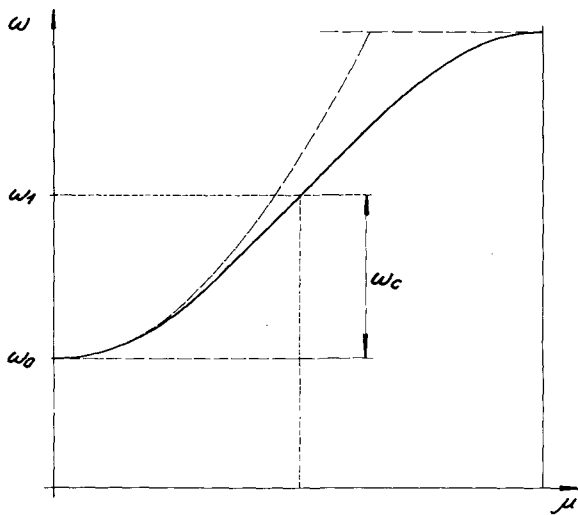


Fig. 7 - Dispersion curve for a periodic structure.

"cut-off" frequency ω_0 for this corrected radius $a + \delta/2$ and the natural decay time-constant τ one obtains the general equation

$$\frac{c^2}{K} \frac{\partial^2 f}{\partial x^2} - \frac{\partial^2 f}{\partial t^2} - \omega_0^2 f - 2/\tau \frac{\partial f}{\partial t} = 0 \quad [10]$$

where the coefficient c^2/K represents the curvature of the dispersion characteristics near cut-off (see Fig. 2); by a proper choice of K (in addition to ω_0 and τ) it is thus possible to fit this equation to the experimental curve near cut-off of an actual structure. Values of K ranging from 1,25 to 2,7 according to geometry are observed; K is high for low energies.

c) Infinite line

Equation [10] is of the telegraphy type and can be solved. Assuming that $f(x, t)$ is given at the input end ($x = 0$), and is zero for negative t , one has:

$$f(x_0, t_0) = \frac{c}{\sqrt{K}} \frac{\partial}{\partial x_0} \int_{|x_0|/\sqrt{K/c}}^{t_0} f(0, t_0 - t) e^{-t/\tau} \cdot J_0(\omega) \sqrt{t^2 - \frac{x_0^2}{c^2}} dt \quad [11]$$

This gives $f(x_0, t_0) = 0$ for $t_0 < |x_0|/\sqrt{K/c}$ so that c/\sqrt{K} is the velocity of the wavefront.

The expression [11] is very general and can be applied to any input signal. In order to illustrate it let us consider the response to

$$f(0, t) = (1 - e^{-t/\tau}) e^{j\omega_0 t} \text{ for } t > 0 \quad [12]$$

One gets

$$f(x_0, t_0) = e^{j\omega_0 t_0} [e^X + X\nu_1(t_0/\tau) + X^3/6 \sigma_1(t_0/\tau) \dots - e^{-t_0/\tau}] \quad [13]$$

where

$$X = x_0 \sqrt{K/c} \sqrt{2j} \omega_0/\tau = (1 + j) \zeta \quad \nu_1(t_0/\tau) = 1 - \Phi(\sqrt{t_0/\tau})$$

$$\sigma_1 = \nu_1(t_0/\tau) - \frac{e^{-t_0/\tau}}{\sqrt{\pi t_0/\tau}} \quad \rho(t_0/\tau) = \frac{1}{\sqrt{1 - e^{-t_0/\tau}}} \quad [14]$$

Φ being the error function:

$$\Phi(z) = \int_0^z \frac{e^{-t}}{\sqrt{\pi t}} dt.$$

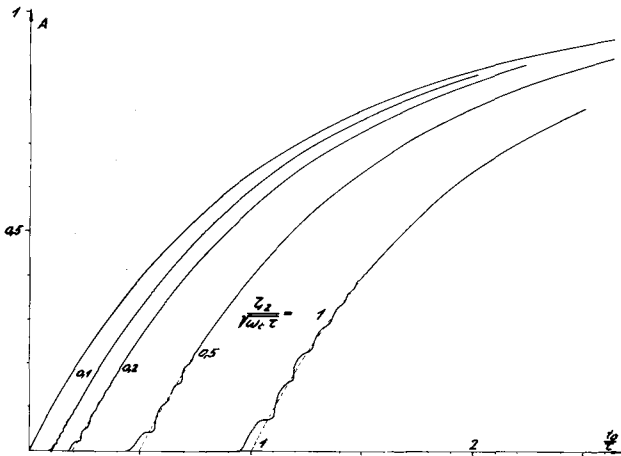


Fig. 8 - Amplitude response along an infinite structure at mid-band (amplitude normalized for $A = 1$ at $t \rightarrow \infty$). Phase is always 0.

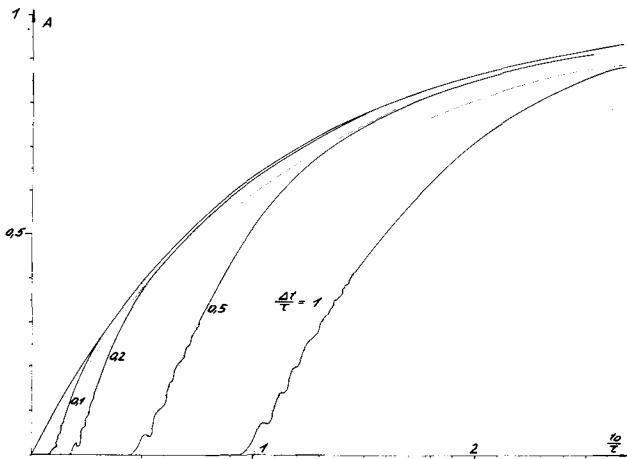


Fig. 9 - Amplitude response at the end of a cavity at mid-band (amplitude normalized for $A = 1$ at $t \rightarrow \infty$). Phase is always 0 or π .

Figs. 3 and 4 show the variations of amplitude and phase as function of time for various values of the parameter $\zeta = x_0 \sqrt{K/c} \sqrt{\omega_0/\tau}$.

They indicate a general delay given by a velocity

$$v \approx \frac{2c}{\sqrt{K} \sqrt{\omega_0 \tau}} = \frac{c}{\sqrt{K}} \sqrt{\frac{2}{Q}} \quad [15]$$

where Q is the Q factor of the structure, and a progressive smoothing out of the signal.

This velocity is rather low for an Alvarez structure.

d) Resonant cavity

For a resonant cavity, made of this waveguide, one obtains approximately

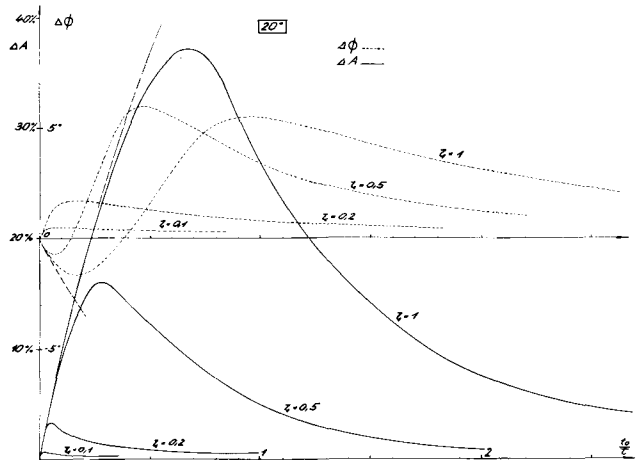


Fig. 10 - Phase and amplitude errors at the end of a zero mode cavity under beam loading conditions for an exact compensation at the feeding point. Beam power equals copper losses; synchronous phase 20° .

$$f(x_0, t_0) = \frac{f(0, t_0)}{\cosh \rho X} \quad [16]$$

where ρ and X are given in [14] and x_0 is the cavity length. Phase and amplitude, as illustrated in Figs. 5 and 6 show now a general response time proportional to x^2 with phase difference and delay which can be expressed by

$$\varphi \approx \frac{\zeta^2 \tau}{t_0} = x_0^2 \frac{K \omega_0}{c^2 t_0} = \omega_0 LC_s \frac{x_0^2}{t_0} \quad \text{and} \quad \Delta t \approx 0,35 \zeta^2 \tau \quad [17]$$

where the equation for φ agrees exactly with [3] and one may see that both φ and Δt are independent of the losses.

4. PERIODIC STRUCTURE MODEL

Practical accelerating structures are always periodic (3). It is of interest to take a dispersion characteristic typical of a periodic structure and check that the above treatment is valid for zero mode and that in the middle of the pass band transient behaviour is governed by the group velocity.

Following the method used by Leiss (4) we take a dispersion equation of the form (see Fig. 7).

$$\omega = \omega_1 + j/\tau - \omega_0 \cos \mu \quad [18]$$

μ being the complex phase shift per cell of length l . This equation exactly fits (10) near zero mode if:

$$\omega_1 = \omega_0 + \omega_c, \quad K = \frac{c^{2 \cdot n}}{l^2 \omega_0 \omega_c}, \quad \text{and} \quad x_0 = ql, \quad [19]$$

q being the number of the cell.

The response of this line to a signal is now given by:

$$f(ql, t_0) = (-1)^{q/2} q \int_0^{t_0} f(0, t_0 - t) e^{j\omega_1 t - t/\tau} J_q(\omega_c t) \frac{dt}{t} \quad [20]$$

and the apparent velocity of the wavefront, dependent on the behaviour of J_q Bessel function, is approximately

$$\frac{c}{\sqrt{K}} \sqrt{\frac{\omega_c}{\omega_0}}$$

a) *Zero mode* - Provided [19] are satisfied, expressions [13] and [14] apply exactly at frequency ω_0 .

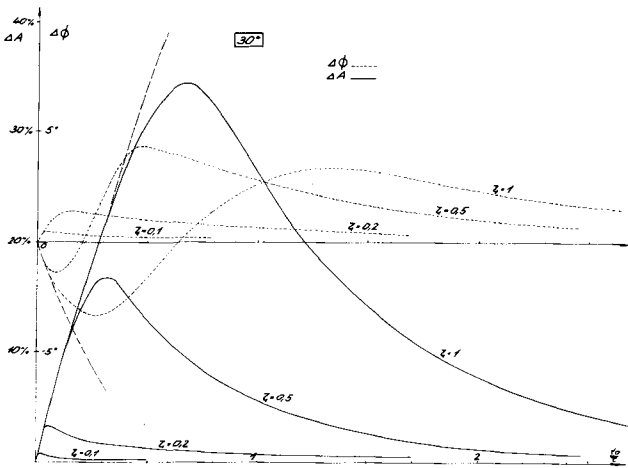


Fig. 11 - Phase and amplitude errors at the end of a zero-mode cavity under beam loading conditions for an exact compensation at the feeding point. Beam power equals copper losses; synchronous phase 30° .

b) *Middle of pass band* - For the case of $\pi/2$ mode [or π mode with resonant coupling (5)] we take frequency ω_1 where phase is constant and amplitude response is shown of Figs. 8 and 9. Signal,

(*) In this case one might argue that for small cell length l and correspondingly large upper cut-off frequency (large ω_c) the constant K increases, as is observed in the Alvarez structure of axially loaded waveguide type (2-3).

wavefront and group velocities are equal. Apart from small undulations at the beginning, the response laws are still similar to zero mode but less distorted (no transient phase shift) and much faster, ζ having to be replaced by

$$\frac{\zeta}{\sqrt{\omega_c \tau}} = \frac{x_0}{l \omega_c \tau} = \frac{\Delta t}{\tau} \quad [21]$$

were Δt is the delay in an infinite line.

5. BEAM LOADING PHENOMENA

a) Induced field

When a bunched beam travels along an accelerating structure it excites a field which tends to decrease the accelerating one. Usually the time taken for the beam to fill the length of the cavity is short enough, compared with the time-constant or filling time of the cavity, to be neglected. The negative transient, induced by beam loading, has therefore a build-up of pure exponential type with no phase nor amplitude delay along the cavity (provided beam phase is the same all the way along).

b) Compensation

Under this assumption sections 2 and 3 show that phase and amplitude delays will occur when compensating this beam loading field by extra power fed in at one point.

If the compensation is exact at the input point, amplitude and phase errors at the end of the cavity are, to a first approximation, proportional to the current. Figs. 10 and 11 show in the case of a zero mode cavity the errors due to a beam loading field equal to the accelerating field for various values of the parameter ζ . Both ζ and the beam-loading field depend on the losses, but in such a way that to good approximation the errors are independent of τ .

6. CONCLUSIONS

It is clear that in order to have the possibility of high current acceleration small values of ζ have to be used ($\zeta < 0,2$ for instance). This requires short lengths and low values of K (which depends in an unknown way on the geometry). However, if a $\pi/2$ mode or resonant-coupled π mode is used, much longer lengths are still satisfactory provided, according to [21], that the pass band and the time-constant (or Q factor) are large enough.

REFERENCES

- (1) H. G. Hereward: Some examples of energy flow in the Alvarez structure. CERN Report MPS/DL Int. 65-1 (1965).
- (2) P. Lapostolle: Phénomènes transitoires dans un guide d'ondes électromagnétiques au voisinage de la fréquence de coupure. Application à la structure Alvarez des accélérateurs linéaires à protons. CERN Report AR/Int. SG/65-9 (1965).
- (3) P. Lapostolle: Phénomènes transitoires dans une structure périodique. Comparaison des modes 0 et π . Application à des structures d'accélérateurs linéaires à protons. CERN Report AR/Int. SG/65-12 (1965).
- (4) J. E. Leiss and R. A. Schrack: Transient and beam loading in Linear Electron Accelerators, N.B.S. Report (1962).
J. E. Leiss: Beam loading in Linear Accelerators. Particle Accelerator Conference. IEE Trans. on Nuclear Science. NS-12 p. 566 (1965)
- (5) E. Knapp: 800 MeV RF structures, 1964 Linear Accelerator Conference. MURA report N.o 714 p. 55.